Environ. Sci. Technol. **2006**, *40,* 4956−4960

Evidence for Oligomer Formation in Clouds: Reactions of Isoprene Oxidation Products

KATYE E. ALTIERI,*,† ANNMARIE G. CARLTON,‡ HO-JIN LIM,‖ BARBARA J. TURPIN,‡ AND SYBIL P. SEITZINGER†,§

Institute of Marine and Coastal Sciences, Department of Environmental Sciences, Rutgers NOAA CMER Program, Rutgers, The State University of New Jersey, New Brunswick, New Jersey 08901-8521, Department of Environmental Engineering, Kyungpook National University, 1370 Sankyuk-dong, Buk-gu Daegu 702−701 Korea

Electrospray ionization mass spectrometry (ESI−MS) was used to investigate product formation in laboratory experiments designed to study secondary organic aerosol (SOA) formation in clouds. It has been proposed that water soluble aldehydes derived from aromatics and alkenes, including isoprene, oxidize further in cloud droplets forming organic acids and, upon droplet evaporation, SOA. Pyruvic acid is an important aqueous-phase intermediate. Time series samples from photochemical batch aqueous phase reactions of pyruvic acid and hydrogen peroxide were analyzed for product formation. In addition to the monomers predicted by the reaction scheme, products consistent with an oligomer system were found when pyruvic acid and OH radical were both present. No evidence of oligomer formation was found in a standard mix composed of pyruvic, glyoxylic, and oxalic acids prepared in the same matrix as the samples analyzed using the same instrument conditions. The distribution of high molecular weight products is consistent with oligomers composed of the mono-, oxo-, and di-carboxylic acids expected from the proposed reaction scheme.

Introduction

Atmospheric particulate matter (PM) scatters and absorbs light, affecting the global radiation budget and climate (*1*). Additionally, exposure to PM is associated with adverse health affects in humans (*2*). A fraction of organic PM, secondary organic aerosol (SOA), is formed by oxidation of reactive organic gases and the subsequent partitioning of low to semi volatile products into the particle phase (*3*). On an annual basis SOA contributes roughly 10−50% of total organic PM in urban areas and as much as 80% during the afternoon hours of ozone episodes (*4*−*6*). The vast majority of SOA research has been devoted to elucidating pathways and yields for homogeneous gas-phase reactions that produce SOA. SOA and oligomer formation through acid-catalyzed aerosol phase reactions has also been documented in smog chamber experiments (*7*−*12*). Oligomer formation might explain the presence of large multifunctional compounds that have long been known to dominate particulate organic mass (e.g., organics not eluted from the GC column; ref *13*).

In addition to homogeneous reactions and aerosol-phase reactions, it has been proposed that, like sulfate, SOA can form through cloud processing (*14*−*17*). Briefly, high hydroxyl radical concentrations in the interstitial spaces of clouds oxidize reactive organics to form highly water soluble compounds (e.g., aldehydes). These compounds partition into cloud droplets where they oxidize further to form less volatile organics (e.g., oxalic acid). When the cloud droplets evaporate, the low volatility organics remain, in part, in the particle phase, yielding SOA. To our knowledge, oligomerization reactions have not previously been observed or shown to form through cloud processing. Should they form, they could substantially enhance in-cloud SOA yields.

In-cloud SOA production from alkenes and aldehydes, including isoprene, has been modeled by Ervens et al. and Lim et al. (*16, 17*). In the chemical mechanism used by Lim et al. (*17*), gas-phase isoprene oxidation produces water-soluble compounds, glycolaldehyde, glyoxal, and methyl glyoxal. These products dissolve into cloud water and react with OH radicals to form oxalic acid, glycolic, and glyoxylic acids via pyruvic and acetic acids (Figure 1).

Methylglyoxal and pyruvic acid are important intermediates in in-cloud reactions of many reactive organics. To ascertain the fate of pyruvic acid, photochemical batch aqueous-phase reactions of pyruvic acid and OH radical were performed. Identified products were consistent with those suggested by Stefan and Bolton (*18*) and used by Lim et al. (*17*) as reported in detail by Carlton et al. (*19*). This work will show that oligomer formation may be an important step omitted in the Lim et al. (*17*) pathway. If reactions that lead to oligomer products are included in the Lim et al. (*17*) pathway it could add substantially to the SOA formed.

Materials and Methods

Experimental Setup. Photochemical, batch aqueous-phase reactions of pyruvic acid and hydrogen peroxide (H_2O_2) were conducted in 1 L borosilicate vessels with quartz immersion wells under conditions encountered by cloud water (pH 2.7−3.1) for 202 min. The reaction vessels were wrapped in aluminum foil to minimize the influence of ambient UV. Low-pressure UV lamps with spectral irradiance at 254 nm were used in the experiments to produce hydroxyl radical from hydrogen peroxide for pyruvic acid oxidation. Three types of control experiments were conducted: (1) a UV control (i.e., pyruvic acid and H_2O_2), (2) a H_2O_2 control (i.e., pyruvic acid and UV), and (3) an organic control (i.e., UV and H_2O_2). Three experiments were conducted, two with pyruvic acid concentrations of 10 mM and H_2O_2 concentrations of 20 mM, and one with the concentrations doubled. A 0.5% catalase solution was added to all experiment and control samples right after sampling to prevent further reaction. Samples were stored frozen until analysis. More detail on experimental setup, sampling, and HPLC procedures can be found in ref *19*.

Analytical Determinations. The ESI−MS analysis was conducted using an HP-Agilent 1100 liquid chromatograph/mass spectrometer consisting of an autosampler and quadrupole mass-selective detector equipped with an atmospheric pressure electrospray ionization source. The autosampler injects samples and standard solutions (20 μL) from individual vials into the LC system. The instrument was run with no column attached, a mobile phase, 60:40 v/v 100% methanol and 0.05% formic acid in deionized water, with a flow rate

* Corresponding author e-mail: altieri@marine.rutgers.edu.
† Institute of Marine and Coastal Sciences, Rutgers University.
‡ Department of Environmental Sciences, Rutgers University.
§ Rutgers NOAA CMER Program, Rutgers University.
‖ Kyungpook National University.

10.1021/es052170n CCC: $33.50
Published on Web 07/13/2006

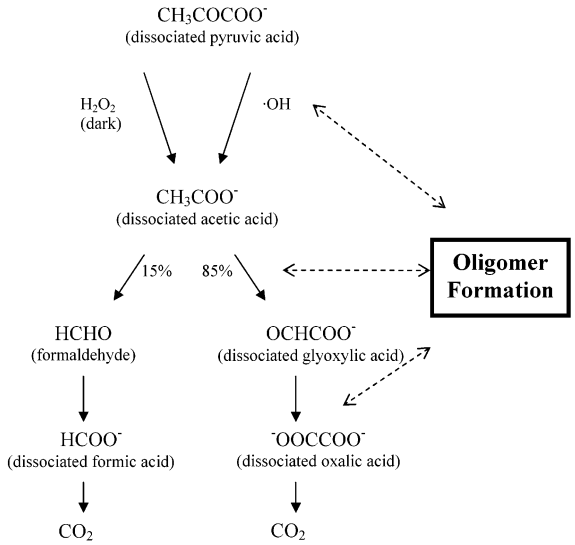

FIGURE 1. Mechanism of oxalic acid formation through isoprene cloud processing. Modified from refs *17, 19* to focus on the pyruvic acid pathway and to include oligomer formation.

of 0.220 mL min^{-1}. The ESI−MS measurements were made in the negative mode over the mass range 50−1000 amu with a fragmentor voltage of 40 V unless otherwise noted. Nitrogen was the drying gas (350 °C, 10 L min^{-1}, 25 psig.). The capillary voltage was 3 kV. The electrospray ionization full-scan mass spectra (m/z 50−1000) with unit mass resolution was recorded on Agilent software (Chemstation version A.07.01) and exported to EXCEL and ACCESS (Microsoft, Inc.) for statistical analysis and interpretation.

Authentic individual and mixed standards of pyruvic, glyoxylic, acetic, formic, and oxalic acids, all expected precursors or products (*17*) (Figure 1), were analyzed using the same instrument conditions as the sample analysis described above. The standard mix used for calculating concentrations in the samples was composed of pyruvic, glyoxylic, and oxalic acids in the same matrix as the samples in the reaction vessels (H_2O_2 at a 1:2 ratio and 1 μL of catalase). The standard mix was analyzed over the range of concentrations (0.025−1.5 mM) typical of the samples, and a standard curve was created for each compound (Table 1). Acetic acid was not included in the standard mix because the ESI−MS did not detect it in either the monomer or dimer form. Previous analysis of samples including acetic acid in the standard mix did not result in the detection of any new ions, nor did it significantly affect the ion abundances of the other compounds in the standard mix. Formic acid has a molecular weight (MW48) below the detection limit of the instrument (m/z 50) and was not detected in either positive or negative mode ESI−MS analysis.

The standard and sample data from the ESI−MS were analyzed using a previously established method (*20*). For each standard and time series sample, six replicate injections were made. The mean ion abundance (±SD) for each m/z in each sample was calculated for the standards and samples. Each mass-to-charge (m/z) with an abundance statistically different from zero at the 0.05 level (*t*-test; ref *21*) was retained. The samples and standards were corrected for deionized blanks by subtracting the ion abundance of any m/z found in the deionized water from the same m/z in standards and samples.

ESI−MS is a soft ionization method that does not fragment ions (*22*). The technique can be applied to any species that can be protonated or deprotonated. Large compounds that would be fragile to fragmentation in other mass spectrometers are analyzed intact by the ESI−MS, including peptides and proteins (*23*). ESI−MS provides molecular weight information as mass-to-charge ratios (m/z) with unit mass resolution. In the negative mode acidic functional groups lose an H^+ and appear at an m/z of the molecular weight minus one $[M-H]^-$.

The fragmentor voltage on the instrument is usually set at 40 V to keep compounds intact. However, for analysis of a subset of samples, the fragmentor voltage was varied. First, the standard mixture of monomers was analyzed with varying fragmentor voltages (40−100 V). Then the time series samples, diluted (1:10) with deionized water, were analyzed at fragmentor voltages 40−100 V to fragment the oligomers that had been formed by the cloud water reactions.

Results and Discussion

Standard Analysis. Pyruvic acid was detected in the negative mode as both the monomer (m/z 87) and homogeneous dimer (m/z 175) forms in authentic standards ($[M-H]^-$, $[2M-H]^-$). Glyoxylic (m/z 73) and oxalic (m/z 89) acids were detected in the monomer form only ($[M-H]^-$, Figure 2), which is consistent with other carboxylic acids in single and mixed standards. Oxalic, glyoxylic, and pyruvic acids were linear up to approximately 1.5 mM (Table 1, Figure 3). However, the slopes differ due to the relationship of ion abundance to concentration being compound dependent.

Sample Analysis. The ion abundance representing pyruvic acid decreased and glyoxylic and oxalic acids increased during the experiment as predicted by Lim et al. (*17*) and discussed by Carlton et al. (*19*) (Figure 4). The ion abundance of the reactant pyruvic acid (m/z 87, 175) decreased from time 44 s to 10 min, and then remained relatively constant throughout the experiment. The intermediate glyoxylic acid (m/z 73) increased in ion abundance slightly from 10 to 27 min (3971 to 4678 units) and then steadily decreased in abundance for the remainder of the reaction to a final abundance of 758 units. The expected product oxalic acid (m/z 89) increased in ion abundance throughout the experiment (Figure 4) and became the dominant peak in the spectrum after 202 min showing good agreement with the proposed mechanism (*17*).

Oligomer Formation. If the time series samples were composed only of the monomers predicted by Lim et al. (*17*), the ESI−MS spectrum should resemble the spectrum of the standard mix of reaction components (Figure 2). However, after 10 minutes of photochemical oxidation, ions higher in molecular weight than the monomers appear in the time series spectrum (Figure 4a) in addition to the monomers predicted by Lim et al. (*17*). The distribution of these higher molecular weight ions in the spectrum at 10 minutes is not completely regular, but appears to be consistent with the development of an oligomer system (Figure 4a). The two peaks with the highest ion abundance in the spectrum are m/z 147 and m/z 217. The most dominant mass species (m/z 147) has tentatively been identified (based on the molecular weight combinations) as a pyruvic and acetic acid dimer.

The spectral complexity increases with time in samples from the photochemical oxidation of pyruvic acid. There are six peaks that dominate the spectrum after 202 min of oxidation (Figure 4b). The most dominant peak is m/z 89, oxalic acid monomer. The following five ions with the next highest abundances after m/z 89 are 103, 133, 147, 177, and 217. The six peaks differ by 14, 30, 14, 30, and 40 amu, respectively. These six ions represent almost half of the total ion abundance of the entire sample. The other half of the total ion abundance in the sample is present in a pattern that is consistent with an oligomer system (Figure 4b). The oligomer haystacks show a highly regular pattern of mass differences of m/z 12, 14, and 16 in the mass range 80−500 amu, and the peaks within the haystacks are separated by 2 amu (Figure 4b). If the mixed acid oligomers in the sample spectra were artifacts of the ESI−MS, they should also appear

TABLE 1. Response of ESI−MS to Compounds in the Standard Mix Composed of the Same Matrix as the Samples in Units of Ion Abundance Per mM Compound.[a]

compound	molecular formula	molecular weight	a	y_0	r^2
pyruvic acid[b]	$CH_3COCOOH$	88.1	472,400	25,630	0.9753
pyruvic acid[c]	$2(CH_3COCOOH)$	176.2	95,130	3,032[d]	0.9847
glyoxylic acid	OCHCOOH	74.0	47,960	6,999	0.8083
oxalic acid	HOOCCOOH	90.0	647,820	−690[d]	0.9997

[a] The r^2 values and equations are calculated from linear regression analysis based on the ion abundance of the mixed standards as a function of concentrations 0.025−1.5 mM; a =slope of the line and $y_0 = y$ intercept. [b][M−H]$^-$ [c] [2M−H]$^-$ [d] Not significantly different than zero $t_{0.05,\ 3}$.

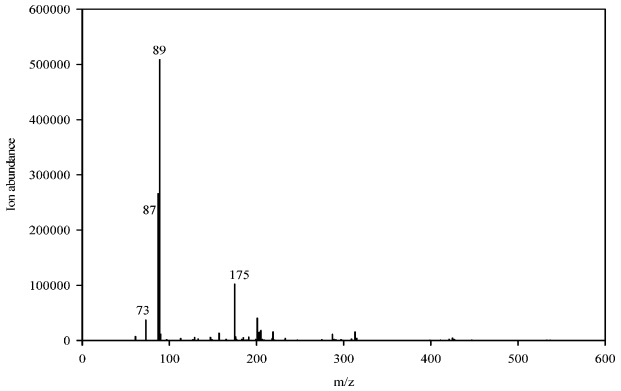

FIGURE 2. Abundance of pyruvic acid monomer (*m/z* 87) and dimer (*m/z* 175), glyoxylic acid (*m/z* 73), and oxalic acid (*m/z* 89) in a 1.5 mM per compound mixed standard in the same matrix as the samples, detected in negative ionization mode with ESI−MS.

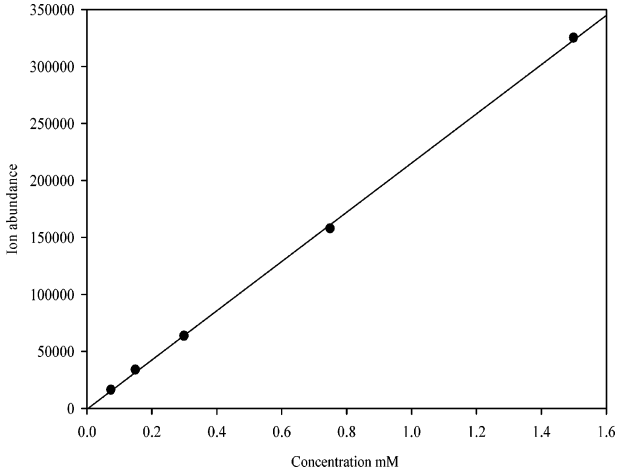

FIGURE 3. ESI−MS response (ion abundance) to oxalic acid (*m/z* 89) in a mixed standard that included pyruvic and glyoxylic acids in the same matrix as the samples across a range of concentrations (0.075−1.5 mM compound) $r^2 = 0.9997$, $y = 647\ 820x - 690$.

in the mixed standard spectra (Figure 2) where all of the reaction components are present; however, they do not. They also do not appear in the control spectra (see below), implying that the formation of oligomers in the samples requires the presence of pyruvic acid and OH radical.

The main peaks in the haystacks can be accounted for by linear combinations of known monomer units, formic, acetic, pyruvic, glyoxylic, and oxalic acids. For example, the gain of 14 could be attributed to the addition of a glyoxylic acid (MW74) instead of an acetic acid (MW60), or the addition of a pyruvic acid (MW88) instead of a glyoxylic acid. The mass difference of 16 could be attributed to adding an oxalic acid (MW90) instead of a glyoxylic acid. The regular distribution of the six dominant ions, the regularity of the lower abundance peaks, and the linear combinations of monomer

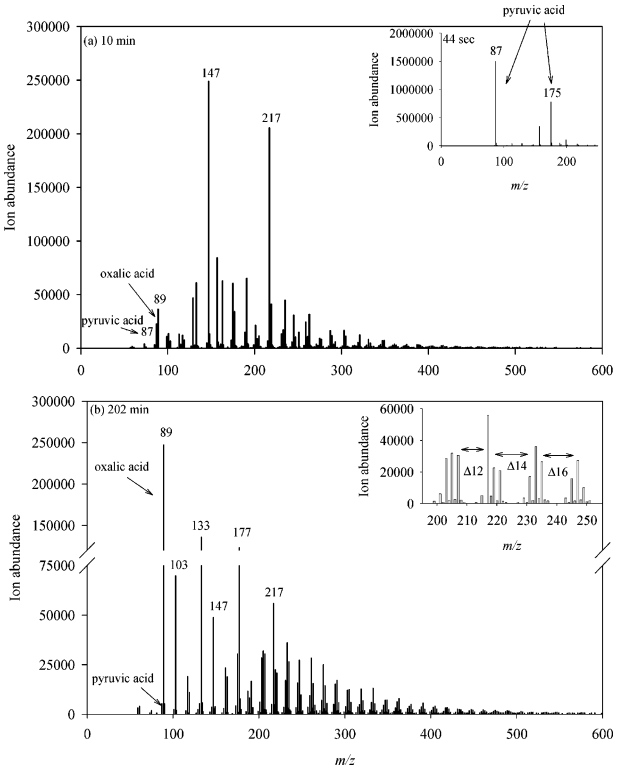

FIGURE 4. ESI−MS spectra of time series samples from pyruvic acid UV/H_2O_2 oxidation after (a) 10 min, and (b) 202 min. Pyruvic acid (*m/z* 87, 175) is the main compound present in a 44 s time series sample from a replicate experiment (inset a). The regular distribution of *m/z* 12, 14, 16 indicating the oligomeric system is shown for an enlarged portion of (b) in the inset. Note break in *y*-axis scale.

units support the presence of an oligomer system (*24*−*26*). This evidence is also consistent with a polydisperse copolymer system (*26*). An important next step is to identify the exact composition of each of the oligomers in the system. The experiments were conducted in the aqueous phase at pH values typical of clouds to simulate cloud chemistry and thus provide evidence that oligomer formation could be occurring under conditions encountered in clouds.

Control Experiments. The formation of the oligomer system requiring the presence of pyruvic acid and the OH radical is supported by the mixed standards (as discussed above) and the two control experiments. When pyruvic acid is exposed in the controls to UV alone or H_2O_2 alone there are additional peaks in the spectra that are not present in the mixed standard. The peaks in the control spectra are not as regular or dense as those in the time series reaction spectra. It is known that pyruvic acid will react to some degree with UV alone (e.g., formic and acetic acids (*19*)). However, the extent of reaction in the control with UV alone is much less than when the pyruvic acid is exposed to UV plus H_2O_2. The pyruvic acid (*m/z* 87, 175) (after approximately 161 min of exposure to UV) is 42% of the total ion abundance, as

TABLE 2. Comparison of the Percent Change in Ion Abundance of Standards as Fragmentor Voltages Increased (40−80 V) to the Percent Change in Ion Abundance of the Samples as Fragmentor Voltages Increased (40−80 V)

	% change 0.5 mM standard	% change 1.0 mM standard	% change $t_{3\ 27\ min}$	% change $t_{6\ 86\ min}$
pyruvic acid	−88	−87	557	825
glyoxylic acid	−67	−65	61[a]	179[a]
oxalic acid	−98	−97	−77	−81

[a] $t_{g1} = 21$ and $t_{g2} = 59$ min sample from replicate experiment due to insufficient sample volume.

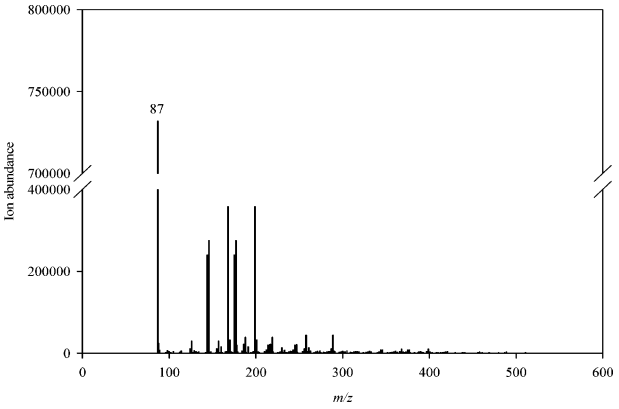

FIGURE 5. ESI−MS spectrum of the UV degradation of pyruvic acid (no H_2O_2 added) after 161 min. Pyruvic acid (*m/z* 87) is present as the most abundant compound and there is a higher molecular weight cluster that is not representative of an oligomer system.

compared to ~2% of the total ion abundance when oxidized by the OH radical. The lack of regularity and density in the control spectra supports the conclusion that pyruvic acid and the OH radical are required for the regularly distributed oligomer system to form. However, compounds formed from the reaction of pyruvic acid and UV alone may be atmospherically relevant and warrant further investigation.

Oligomer Quantification. The goal of changing the fragmentor voltage when analyzing standards and samples was to see if the potential monomer constituents increased in abundance as the larger molecular weight compounds were broken apart. This would provide additional evidence that these high molecular weight compounds are oligomers. In the mixed monomer standards, as the fragmentor voltage increased, the monomer ion abundances $[M-H]^-$ decreased as expected as the compounds were fragmented (Table 2, Table S-1a−c, Figure 6). The fragmented components smaller than *m/z* 50, which is the lower mass detection limit of the instrument, are not detected.

For the sample analysis, the percent of initial monomer abundance that should be lost by increasing the fragmentor voltage was known from the standard analysis. In contrast to the standards decreasing in ion abundance, the monomers (pyruvic and glyoxylic acid) in the samples initially increased in abundance as fragmentor voltage increased (Figure 6, Tables S-1a−c). This *increase* in abundance implies that a larger molecular weight compound was breaking apart and contributing to the monomer abundance. The oxalic acid monomer decreased in ion abundance with increased fragmentor voltage in the samples, but this decrease was 20% less than the standard decrease. The decrease in abundance from fragmentation seen in the standards was overwhelmed in the samples by an increase in abundance from fragmentation of higher molecular weight species. This is consistent with the decrease in abundance in the higher

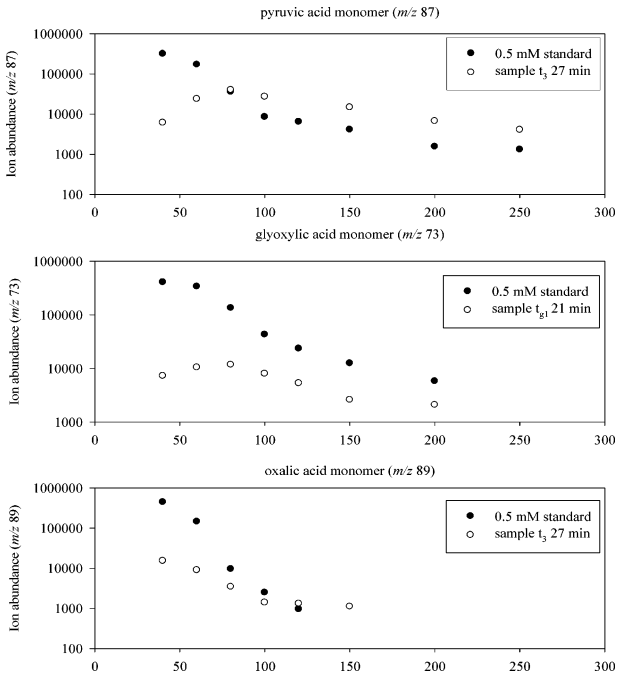

FIGURE 6. Response (ion abundance) of pyruvic acid (*m/z* 87), glyoxylic acid (*m/z* 73), and oxalic acid (*m/z* 89) to varying fragmentor voltages in a 0.5 mM mixed standard (filled circles) and time series samples (empty circles).

molecular weight compounds as the fragmentor voltage was increased. Thus, the larger molecular weight oligomers are at least partially composed of the known monomers, pyruvic acid, glyoxylic acid, and oxalic acid.

The increased monomer abundance in the samples with increased fragmentor voltage, in contrast to the decrease in the standard monomer abundance, was used to estimate the concentration of monomer present in the oligomers. The percent of monomer lost with increased fragmentor voltage for the standards is concentration independent (Table 2). For example, the 0.5 mM mixed standard was used to determine the percent loss of glyoxylic acid (*m/z* 73) in ion abundance (67%) as the fragmentor voltage was increased from 40 to 80 V (Table 2). In sample t_{g1} (sample from a replicate experiment due to insufficient sample volume) glyoxylic acid (*m/z* 73) had an abundance of 7284 units (Table S-1b). After increasing the fragmentor voltage to 80 V, fragmentation alone would have decreased the glyoxylic acid (*m/z* 73) ion abundance by 67% to 2404 units. In sample t_{g1}, the glyoxylic acid (*m/z* 73) actually increased in ion abundance to 11 755 units (Table S-1b). Thus 9351 units of glyoxylic acid were generated by fragmentation of oligomers. This increase in ion abundance, the glyoxylic acid response factor (Table 1), and the dilution factor (1:10) were used to calculate that at least 0.49 mM of glyoxylic acid was present in the oligomers in the t_{g1} sample, and 0.85 mM in the t_{g2} sample.

The concentration of monomers from oligomer breakup was calculated as described above for pyruvic and oxalic acids. The pyruvic acid calculated to be in oligomers is 0.29 mM in sample t_3. The oxalic acid calculated to be in oligomers is 0.06 mM for sample t_3 and 0.09 mM in sample t_6. For sample t_3, there is approximately the same amount of oxalic acid present as a monomer (0.04 mM) (Table S-2) as there is present in oligomers (0.06 mM). As the reaction proceeds, sample t_6 has more oxalic acid present in its monomer form (0.30 mM) (Table S-2) than it does in oligomers (0.09 mM). The concentration of oxalic acid monomer increases with time (Figure 4) but the concentration of oxalic acid in oligomers increases very little in comparison to the monomer increase from sample t_3 to t_6.

This work is the first time that evidence for oligomer formation in cloud processing reactions has been reported. The presence of the reaction components as oligomers instead of only monomers is likely to have important implications to in-cloud SOA formation. The oligomer forms will have lower vapor pressures and will remain to a much larger extent in the particle phase after cloud evaporation than the monomers. Also, oligomer formation from reaction products may enhance the effective Henry's law constants for precursor aldehydes, further enhancing SOA. It is possible that the absorptive and scattering properties of clouds and of particles could be altered by the presence of oligomers since some large multifunctional compounds believed to be formed in the atmosphere have some associated absorption (*27*). Thus in-cloud oligomer formation could have an effect on radiative forcing.

There remain many unanswered questions about the potential effect of oligomers formed through cloud processing. These experiments are consistent with oligomers forming through irreversible reactions. However, the laboratory experiments are conducted in a closed system, while the atmosphere is an open system which allows partitioning. The behavior of oligomers upon droplet evaporation is yet unknown. Oligomers formed through in-cloud aqueous-phase reactions could contribute to the concentration of surfactants observed in cloud droplets (*28*); however, it is not clear whether surfactant formation through this pathway will be great enough to substantially alter surface coverage, droplet surface tension, and gas exchange. An important next step is to parametrize oligomer formation for SOA modeling.

Acknowledgments

This research has been supported by a grant from the U.S. Environmental Protection Agency's Science to Achieve Results (STAR) program (grant R831073). Although the research described in this paper has been funded wholly or in part by the U.S. Environmental Protection Agency's STAR program, it has not been subjected to any EPA review, and therefore, does not necessarily reflect the views of the Agency, and no official endorsement should be inferred. We also thank Ron Lauck.

Supporting Information Available

Organic acid responses in ion abundance to varying fragmentor voltages in standards and samples (Tables S-1a−c). Concentrations of organic acid monomers based on ESI−MS ion abundances (Table S-2). This material is available free of charge via the Internet at http://pubs.acs.org.

Literature Cited

(1) IPCC. *Climate Change: The scientific basis*; Cambridge University Press: Cambridge, UK, 2001.

(2) EPA. *Air quality criteria for particulate matter*, 1; U.S. Government Printing Office: Washington, DC, 2004.

(3) Seinfeld, J. H.; Pankow, J. F. Organic atmospheric particulate material. *Annu. Rev. Phys. Chem.* **2003**, *54* 121−140.

(4) Turpin, B. J.; Huntzicker, J. J. Identification of Secondary Organic Aerosol Episodes and Quantitation of Primary and Secondary Organic Aerosol Concentrations During Scaqs. *Atmos. Environ.* **1995**, *29* (23), 3527−3544.

(5) Polidori, A.; Turpin, B. J.; Lim, H. J.; Cabada, J. C.; Subramanian, R.; Robinson, A. L.; Pandis, S. N. Local and regional secondary organic aerosol: Insights from a year of semi-continuous carbon measurements at Pittsburgh. *Aerosol Sci. Technol.* 2005.

(6) Turpin, B. J.; Saxena, P.; Andrews, E. Measuring and simulating particulate organics in the atmosphere: problems and prospects. *Atmos. Environ.* **2000**, *34* (18), 2983−3013.

(7) Jang, M.; Czoschke, N. M.; Lee, S.; Kamens, R. M. Heterogeneous atmospheric aerosol production by acid-catalyzed particle-phase reactions. *Science* **2002**, *298* (5594), 814−817.

(8) Kalberer, M.; Paulsen, D.; Sax, M.; Steinbacher, M.; Dommen, J.; Prevot, A. S. H.; Fisseha, R.; Weingartner, E.; Frankevich, V.; Zenobi, R.; Baltensperger, U. Identification of polymers as major components of atmospheric organic aerosols. *Science* **2004**, *303* (5664), 1659−1662.

(9) Tolocka, M. P.; Jang, M.; Ginter, J. M.; Cox, F. J.; Kamens, R. M.; Johnston, M. V. Formation of oligomers in secondary organic aerosol. *Environ. Sci. Technol.* **2004**, *38* (5), 1428−1434.

(10) Gao, S.; Ng, N. L.; Keywood, M.; Varutbangkul, V.; Bahreini, R.; Nenes, A.; He, J. W.; Yoo, K. Y.; Beauchamp, J. L.; Hodyss, R. P.; Flagan, R. C.; Seinfeld, J. H. Particle phase acidity and oligomer formation in secondary organic aerosol. *Environ. Sci. Technol.* **2004**, *38* (24), 6582−6589.

(11) Gao, S.; Keywood, M.; Ng, N. L.; Surratt, J.; Varutbangkul, V.; Bahreini, R.; Flagan, R. C.; Seinfeld, J. H. Low-molecular-weight and oligomeric components in secondary organic aerosol from the ozonolysis of cycloalkenes and alpha-pinene. *J. Phys. Chem. A.* **2004**, *108* (46), 10147−10164.

(12) Kanakidou, M.; Seinfeld, J. H.; Pandis, S. N.; Barnes, I.; Dentener, F. J.; Facchini, M. C.; van Dingenen, R.; Ervens, B.; Nenes, A.; Nielsen, C. J.; Swietlicki, E.; Putaud, J. P.; Balkanski, Y.; Fuzzi, S.; Horth, J.; Moortgat, G. K.; Winterhalter, R.; Myhre, C. E. L.; Tsigaridis, K.; Vignati, E.; Stephanou, E. G.; Wilson, J. Organic aerosol and global climate modelling: a review. *Atmos. Chem. Phys. Discuss.* **2004**, *4* 5855−6024.

(13) Rogge, W. F.; Hildemann, L. M.; Mazurek, M. A.; Cass, G. R.; Simoneit, B. R. T. Sources of fine organic aerosol .4. Particulate abrasion products from leaf surfaces of urban plants. *Environ. Sci. Technol.* **1993**, *27* (13), 2700−2711.

(14) Blando, J. D.; Turpin, B. J. Secondary organic aerosol formation in cloud and fog droplets: a literature evaluation of plausibility. *Atmos. Environ.* **2000**, *34* (10), 1623−1632.

(15) Chebbi, A.; Carlier, P. Carboxylic acids in the troposphere, occurrence, sources, and sinks: A review. *Atmos. Environ.* **1996**, *30* (24), 4233−4249.

(16) Ervens, B.; Feingold, G.; Frost, G. J.; Kreidenweis, S. M. A modeling study of aqueous production of dicarboxylic acids: Chemical pathways and speciated organic mass production. *J. Geophys. Res., [Atmos.]* **2004**, *109* D15205-1-20.

(17) Lim, H. J.; Carlton, A. G.; Turpin, B. J. Isoprene forms secondary organic aerosol through cloud processing: Model simulations. *Environ. Sci. Technol.* **2005**, *39* (12), 4441−4446.

(18) Stefan, M. I.; Bolton, J. R. Reinvestigation of the acetone degradation mechanism in dilute aqueous solution by the UV/H_2O_2 process. *Environ. Sci. Technol.* **1999**, *33*, 870−873.

(19) Carlton, A. G.; Turpin, B. J.; Lim, H. J.; Altieri, K. E.; Seitzinger, S. Link between isoprene and secondary organic aerosol (SOA): Pyruvic acid oxidation yields low volatility organic acids in clouds. *Geophys. Res. Lett.* **2006**, *33* (6).

(20) Seitzinger, S. P.; Hartnett, H.; Lauck, R.; Mazurek, M.; Minegishi, T.; Spyres, G.; Styles, R. Molecular-level chemical characterization and bioavailability of dissolved organic matter in stream water using electrospray-ionization mass spectrometry *Limnol. Oceanogr.* **2005**, *50* (1), 1−12.

(21) Sokal, R. R.; Rohlf, F. J. *Biometry*, 2 ed.; Freeman: New York, 1981.

(22) *Electrospray ionization mass specrometry: Fundamentals, instrumentation, and applications*; Wiley: New York, 1997.

(23) Loo, J. A.; Loo, R. R. O. Chapter 11. In *Electrospray Ionization Mass Spectrometry*; Cole, R. B., Ed.; Wiley: New York 1997.

(24) Nielen, M. W. F. Maldi time-of-flight mass spectrometry of synthetic polymers. *Mass Spectrom. Rev.* **1999**, *18* (5), 309−344.

(25) Zoller, D. L.; Johnston, M. V. Microstructures of butadiene copolymers determined by ozonolysis/MALDI mass spectrometry. *Macromolecules* **2000**, *33* (5), 1664−1670.

(26) Cox, F. J.; Johnston, M. V.; Qian, K.; Peiffer, D. G. Compositional analysis of isobutylene/p-methylstyrene copolymers by matrix-assisted laser desorption/ionization mass spectrometry. *J. Am. Soc. Mass Spectrom.* **2004**, *15* (5), 681−688.

(27) Gelencser, A.; Hoffer, A.; Kiss, G.; Tombacz, E.; Kurdi, R.; Bencze, L. In-situ formation of light-absorbing organic matter in cloud water. *J. Atmos. Chem.* **2003**, *45* 25−33.

(28) Decesari, S.; Facchini, M. C.; Mircea, M.; Cavalli, F.; Fuzzi, S. Solubility properties of surfactants in atmospheric aerosol and cloud/fog water samples. *J. Geophys. Res., [Atmos.]* **2003**, *108* (D21).

Received for review October 31, 2005. Revised manuscript received May 30, 2006. Accepted June 15, 2006.

ES052170N